Hindawi
Journal of Nanomaterials
Volume 2020, Article ID 5263042, 10 pages
https://doi.org/10.1155/2020/5263042

Research Article

Determining the Aspect Ratio of Palygorskite by Dynamic Laser Light Scattering and X-Ray Diffraction Analysis Techniques

Fei Xie,[1,2,3,4] Jie Zhang,[1,2,3,4] and Jiyan Chen[5]

[1]*Mining College, Guizhou University, Guiyang 550025, China*
[2]*Key Laboratory of Nonmetallic Mineral Resources Comprehensive Utilization, Guiyang 550025, China*
[3]*Guizhou Engineering Lab of Mineral Resources Guiyang, 550025 Guiyang, China*
[4]*National & Local Joint Laboratory of Engineering for Effective Utilization of Regional Mineral Resources from Karst Areas, Guiyang, 550025 Guizhou, China*
[5]*College of Resources and Environmental Engineering, Guizhou University, Guiyang 550025, China*

Correspondence should be addressed to Jie Zhang; zhj59106@163.com

Received 25 April 2020; Revised 5 September 2020; Accepted 21 November 2020; Published 4 December 2020

Academic Editor: Bo Tan

As a natural two-dimensional nanomaterial, palygorskite has been widely used in the fields of biology, chemical industry, medicine, and agriculture. Recently, more and more researchers point out that the aspect ratio of palygorskite directly affects the properties of its composite materials. Due to the large specific surface area and the tiny width of the palygorskite rod-like particles, it is difficult to obtain the aspect ratio information quickly and accurately by conventional means such as microphotography method and specific surface area method. In this paper, the length and width of the crystal is measured quickly and accurately by using dynamic laser light scattering technique and X-ray diffraction technique, so that the aspect ratio of the crystal can be calculated easily. It is recommended to analyze the crystallite size and microstrain of the diffraction pattern of palygorskite that using Pearson VII function, Caglioti equation, and average (LANGFORD) method, after comparing the three modes of W.-H. method. This feasible method has a good application prospect of the study of rod-like nanomaterials.

1. Introduction

The appearance of granular materials and size determines the performance and use of materials, so it is particularly important to study its size. The aspect ratio is one of the most important morphological features of rod-like and fiber-like materials, which not only determines the rheological properties of such materials [1–3] but also affects its catalytic performance, environment control performance, and drug delivery performance [4]. Palygorskite is a natural rod-like mineral material with internal pore structure, which has excellent stability, adsorbability, and colloid property. Its crystal length is about 0.5-5 μm, and the width is about 20-70 nm [5, 6], as shown in Figure 1. At present, palygorskite has been widely used in biological, chemical, pharmaceutical, agricultural, and other fields [7]. Many researchers have pointed out that the aspect ratio of palygorskite directly affects various properties of composite materials [8–12]. Research on the characterization method of the aspect ratio of palygorskite has not attracted much attention, although it has always been a difficult problem to obtain the accurate information on the aspect ratio of palygorskite. Therefore, this paper applied dynamic laser light scattering (DLS) and X-ray diffraction (XRD) to the study of aspect ratio, in order to find a rapid and accurate characterization method for this problem.

1.1. Common Characterization Methods of Aspect Ratio. The aspect ratio (p) is defined as the ratio of the primary size of the particle to the secondary size [11] (Equation (1)).

$$p = \frac{l}{w}, \tag{1}$$

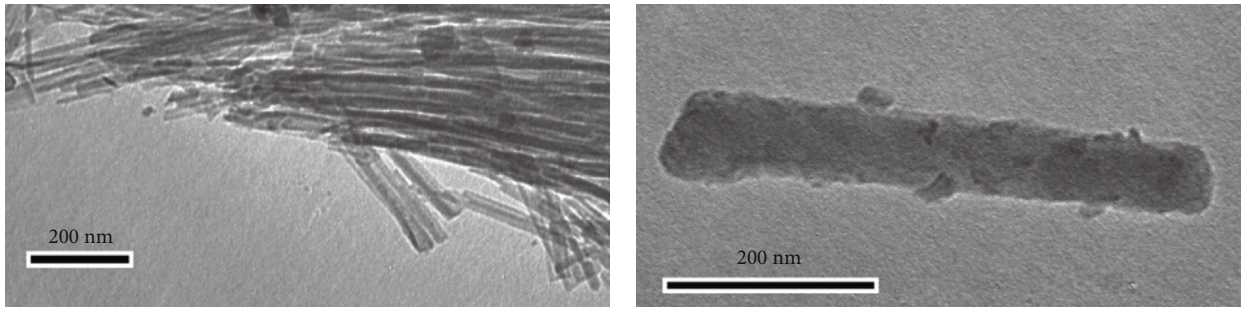

(a) (b)

Figure 1: TEM image of palygorskite crystal ((a) palygorskite crystal beam; (b) single palygorskite crystal).

where p is the aspect ratio, l is the primary particle size (length), and w is the secondary particle size (width).

At present, there are two conventional characterization methods of "aspect ratio". One, called "Specific surface area method," is to calculate the aspect ratio by measuring the particle surface area and particle size distribution [12]. The other, called "microphotography method," is to observe the samples dispersed in the sample rack by using the microscopic imaging technology and then use the image analysis software to measure the length and width of the particles [13]. These methods have their own advantages and disadvantages.

The specific surface area method has a strong theoretical basis, but the specific surface area of particles is always difficult to be measured, especially when analyzing materials with internal pores. So it always deviates from the actual value of aspect ratio.

The microphotography method can accurately measure the length and width of the particles from the microscopic image, so as to quickly obtain the aspect ratio of the samples. However, the measurement accuracy of this method mainly depends on the image resolution. For example, the resolution of the commonly used Noran5 microimage analysis instrument is 22 nm. When the particle size is smaller than this range, a large error will occur. Moreover, image analysis is to analyze a limited number of particles in a limited view field, usually tens to hundreds of particles, so it is difficult to achieve comprehensive particle size statistics [14]. As is known, the diameter of nanomaterial is quite small, only calculated with the diameter of 22 nm, there are 31×10^{12} nanospheres in the range of 1 cm × 1 cm. So it is necessary to improve a method that can characterize a sufficient number of nanoparticles to obtain the accurate length-diameter ratio of the sample particles.

1.2. X-Ray Powder Diffraction and Dynamic Light Scattering. The mineral palygorskite is known to be a long rod-like crystal. The aspect ratio of palygorskite is actually the ratio of the length and the width of the single palygorskite crystal. In this paper, X-ray powder diffraction technique was used to analyze the secondary size, and dynamic light scattering technique (DLS) was used to measure the primary size of palygorskite crystals. Finally, the aspect ratio was obtained by combining the two kinds of crystallite size information. By repeated comparison, the aspect ratio provided by this method well reflected the actual situation.

1.2.1. X-Ray Powder Diffraction (XRD). The analysis of XRD pattern offers important microstructure information about the powder samples, such as crystal structure, microstrain, crystallite size, crystal defect concentration, and distribution [15]. The XRD pattern is generated by a huge amount of crystal particles, often more than 10×10^{13}. The information extracted by XRD analysis is more reliable, compared with other methods. Generally, crystallite size (D) can be calculated by Scherrer Equation (Equation (2)).

$$D_{nkl} = \frac{k\lambda}{\beta \cos \theta}, \tag{2}$$

where D_{HKL} is the crystallite size, K is the crystal shape factor, λ is the wavelength of X-ray, and β is the half peak width of the diffraction peak at the Bragg angle. Equation (2) can be used to calculate the crystallite diameter of D_{hkl} along the direction perpendicular to the crystal plane (HKL) by using the half peak width of the diffraction peak at the Bragg angle.

In order to effectively analyze the XRD pattern and obtain accurate information such as crystallite size and microstrain, the W.-H. method is often used in recent years. The W.-H. method is a simple and easy way to describe the phenomenon of XRD peak broadening, which interprets the peak broadening as a function of crystallite size, microstain and Bragg angle (θ) [16–18]. Equation (3) can be achieved when logarithm is taken from both sides of Equation (2). The crystallite size of the samples can be calculated from the y-intercept of the line fitting in the plots of ln (β) versus ln (1/cos θ). This is the basic principle of the W.-H. method.

$$\mathrm{In}(\beta) = \mathrm{In}\left(\frac{k\lambda}{D}\right) + \mathrm{In}\left(\frac{1}{\cos \theta}\right). \tag{3}$$

After taking the microstrain into account, Equation (3) can be rewritten in three different forms, corresponding to

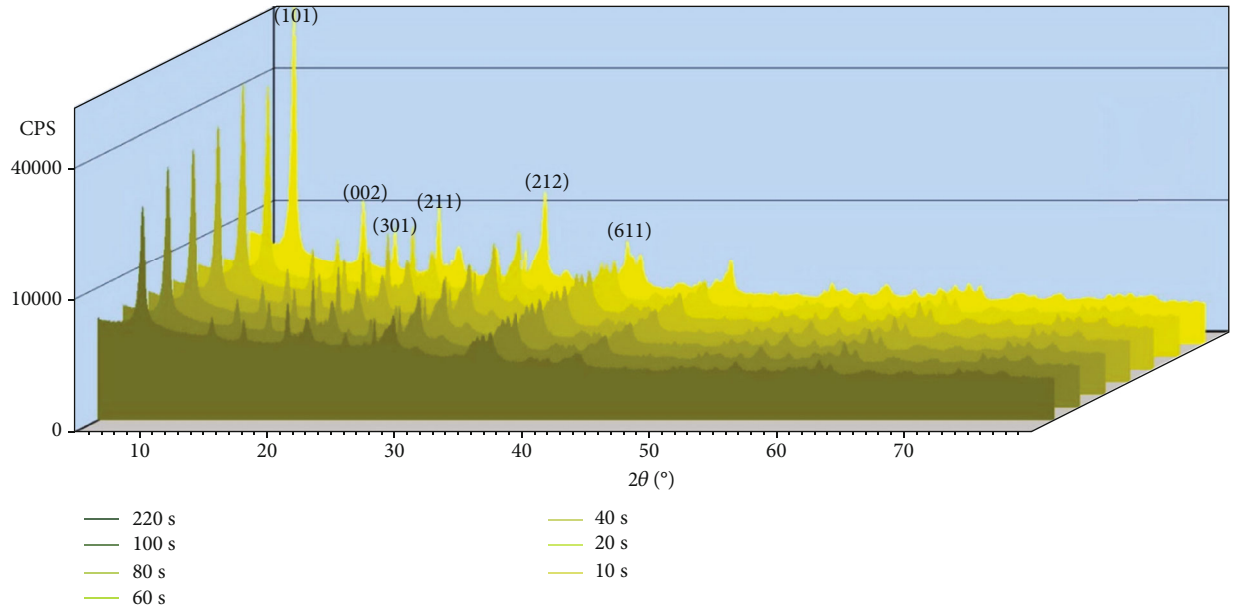

Figure 2: XRD pattern comparison of different grinding time.

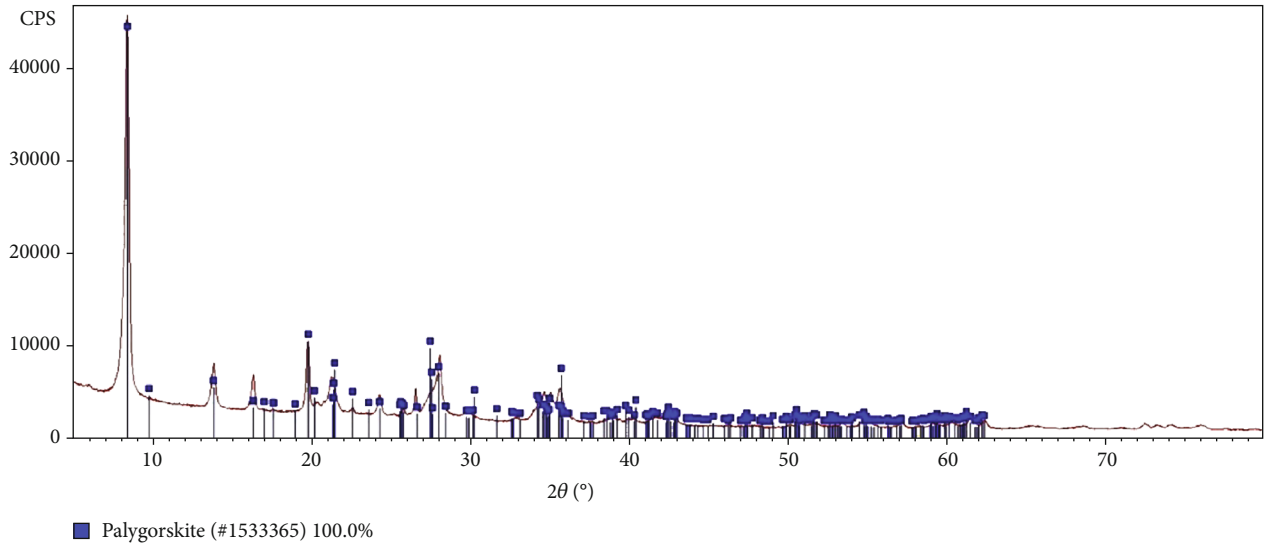

Figure 3: XRD pattern identified by standard card.

Table 1: W.-H. analysis results of palygorskite.

Sample	Grinding time	W.-H. plot crystallite size (nm)			W.-H. plot microstrain (%)		
		Average	Linear	Quadratic	Average	Linear	Quadratic
1	10 s	31.80 ± 0.80	27.80 ± 3.30	25.80 ± 7.20	0.20 ± 0.10	0.04 ± 0.05	0.10 ± 0.10
2	20 s	28.00 ± 0.01	28.60 ± 0.01	25.90 ± 2.70	0.20 ± 0.05	0.09 ± 0.01	0.20 ± 0.04
3	40 s	27.73 ± 0.01	27.20 ± 0.10	26.20 ± 2.30	0.15 ± 0.04	0.03 ± 0.01	0.11 ± 0.03
4	60 s	26.80 ± 0.01	23.70 ± 0.04	24.00 ± 2.80	0.15 ± 0.06	−0.02 ± 0.01	0.00 ± 0.05
5	80 s	26.40 ± 0.01	26.50 ± 0.10	25.60 ± 2.00	0.13 ± 0.04	0.03 ± 0.01	0.11 ± 0.03
6	100 s	25.50 ± 0.10	26.40 ± 0.10	23.60 ± 2.50	0.23 ± 0.05	0.11 ± 0.01	0.24 ± 0.04
7	220 s	22.90 ± 0.20	39.00 ± 2.10	28.20 ± 5.30	0.40 ± 0.20	0.39 ± 0.01	0.52 ± 0.07

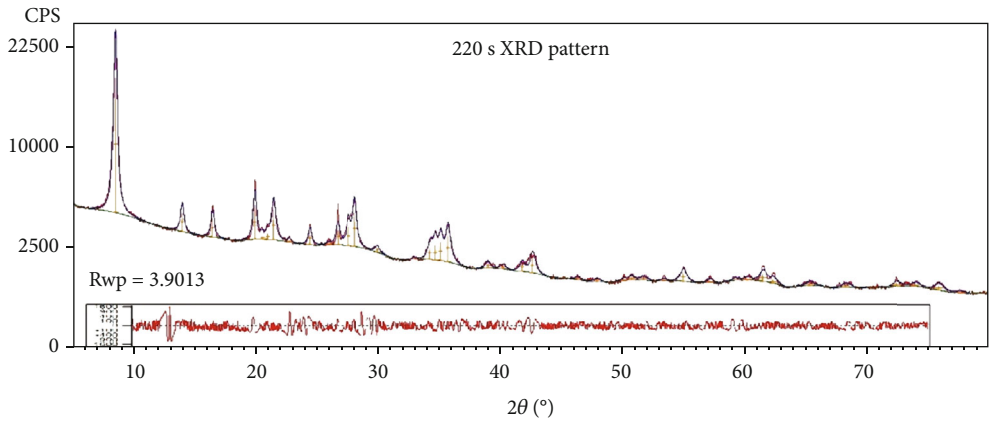

(a)

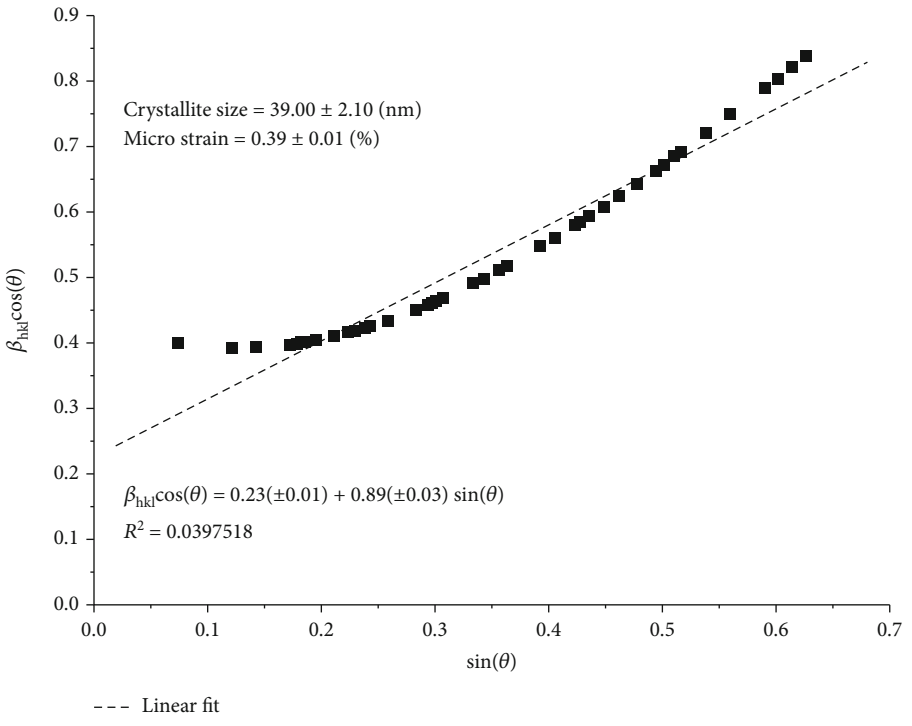

(b)

Figure 4: Continued.

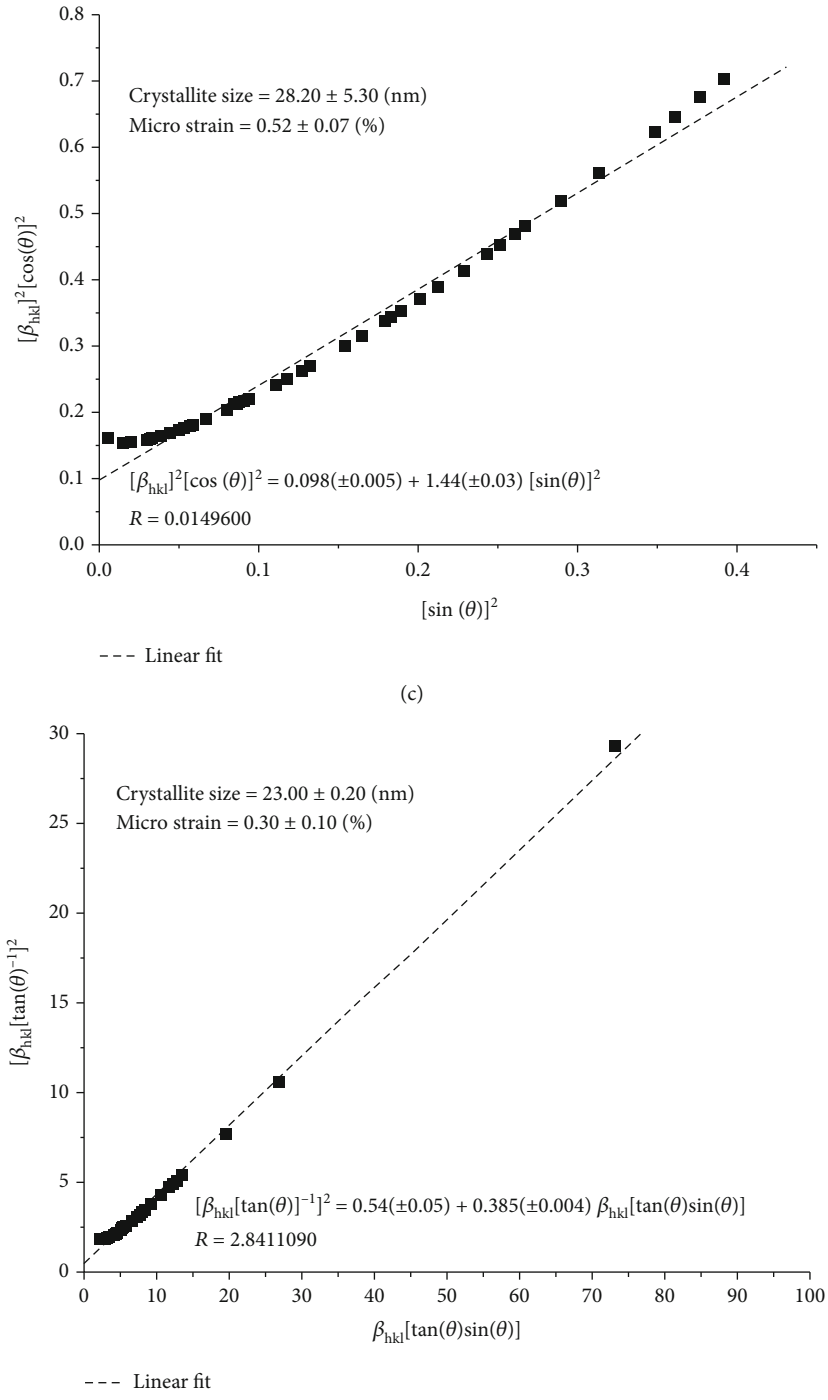

Figure 4: Analysis process of 220 s sample ((a) the XRD pattern; (b) the classic linear W.-H. plot; (c) the quadratic W.-H. plot, (d) the average W.-H. plot).

three W.-H. plot modes. The classical linear W.-H. mode, corresponding to Equation (4), is applicable to the case that the peak broadening only varies with the crystallite size. The quadratic W.-H. mode, corresponding to Equation (5), is suitable for the case that the peak broadening only varies with microstrain. The average W.-H. plot mode, known as the LANGFORD method corresponding to Equation (6), is applicable to the case that the peak broadening varies with the crystallite size and microstrain.

$$\beta_{hkl} \cos\theta = \frac{k\lambda}{\mathrm{D}} + 4\varepsilon \sin\theta, \tag{4}$$

$$\beta_{hkl}^2 \cos^2\theta = \left(\frac{k\lambda}{D}\right)2 + 16\varepsilon^2 \sin^2\theta, \tag{5}$$

$$\frac{\beta_{hkl}^2}{\tan^2\theta} = \frac{\beta_{hkl} k\lambda}{D \times \sin\theta \times \tan\theta} + 16\varepsilon^2, \quad (6)$$

where D is the crystallite size, ε is the microstrain, β_{hkl} is the integral width of the diffraction peak, θ is the Bragg angle, K is the crystal shape factor (generally is 1.00), and λ is the wavelength of Cu-Kα radiation ($\lambda = 0.15406$ nm).

1.2.2. Dynamic Light Scattering (DLS). Dynamic light scattering (DLS) is a characterization method of measuring particle size distribution in solution or suspension [19–21]. Khouri et al. (2014) pointed out that dynamic light-scattering technology can accurately measure the rotation radius (R_g) of nanoparticles within the range of 10-1000 nm [23].

2. Experimental Materials and Methods

2.1. Experimental Materials. The samples used in this paper were collected in Dafang county, Guizhou province, China, which was found to have obvious fiber characteristics [23]. Palygorskite clay was purified and activated by 10% hydrogen peroxide and 10% hydrochloric acid. The purified sample was dried for 3 h at 120°C and then ground into powder with a high-speed vibration mill.

2.2. Experimental Methods

2.2.1. XRD. The X-ray pattern was obtained using X'pert Pro X-ray diffractometer, manufactured by Panalytical. Using Cu cube ($\lambda = 0.15406$ nm) to conduct X-ray diffraction analysis at 40 kV and 40 mA. The pattern was refined with HighScore Plus 4.7 software to obtain accurate crystallite sizes of the sample particles [24].

2.2.2. DLS. Delsa Nano C particle analyzer produced by Beckman Coulter was used to analyze the dynamic light scattering particle size of palygorskite. The analyzer has high precision and reliability and has been widely used to measure the particle size of nanomaterials. The sample was dispersed in 1.0×10^{-3} mol L^{-1} NaCl solution by ultrasound, and a suspension of 1.0 g L^{-1} was prepared. The particle sizes were obtained by repeating the determination in the analyzer for 3 times.

2.2.3. TEM. Gem-2100 transmission electron microscope was used to observe the microscopic morphology. The sample powder was dispersed in anhydrous ethanol solution. After 10 minutes of ultrasonic dispersion, it was dripped to a clean copper network. After being dried, it was used to observe the micromorphology.

3. Results and Discussions

3.1. XRD. X-ray diffraction patterns of palygorskite synthesized from different grinding time are given in Figure 2. All diffraction peaks that are attributed to monoclinic structure space group C 1 2/m1 (12) conform with Crystallography Open Database(COD) data with card number (#1533365) [25] (as shown in Figure 3). The six main planes (101), (002), (301), (211), (212), and (611) of monoclinic phase of palygorskite are observed at $2\theta = 8.505°$, 13.867°, 16.400°, 20.805°, and 27.943°, respectively. Figure 3 clearly shows that the intensity of the diffraction peak of palygorskite decreases with the increase of grinding time, indicating that its grain sizes decrease with the increase of grinding time.

Table 2: Calculation of the aspect ratio of palygorskite crystals.

Sample	Grinding time (s)	Length by DlS (nm)	Width by XRD (nm)	Aspect ratio
1	10.00	1599.50	31.80	50.30
2	20.00	1191.60	28.00	42.56
3	40.00	906.70	27.73	32.70
4	60.00	859.70	26.80	32.08
5	80.00	713.00	26.40	27.01
6	100.00	674.50	25.50	26.45
7	220.00	359.60	22.90	15.70

In this paper, the HighScore Plus4.7 software is used to estimate the crystallite sizes of 7 palygorskite samples prepared in different grinding time. Pearson VII function is used as the peak shape fitting function, Caglitoti equation is used for the FWHM equation, and peak position and area are modified during the fitting process. The calculation results also with the deviation are shown in Table 1.

Taking the 220 s sample as an example, the process of analyzing the palygorskite XRD pattern by means of W.-H. methods was explained in Figure 4. The analysis of other samples was carried out using the same process. Firstly, 41 diffraction peaks of palygorskite crystal were selected, and Pearson VII peak function was used to fit the original pattern, while the fitting error R_{wp} was 3.9013 (as shown in Figure 4(a)). From the fitted peak function, the integral width of each diffraction peak was obtained. Then, the particle size and microstrain were analyzed by three W.-H. plot methods. The classic linear W.-H. plot is shown in Figure 4(b), and the quadratic W.-H. plot is shown in Figure 4(c). The fitting lines were drawn in the two figures, of which the slopes rendered the microstrain, while the offset was used to calculate the crystallite size. The average W.-H. plot was drawn in Figure 4(d). In contrast to the other two methods, the slope of the fitting line rendered the crystallite size, while the offset is used to calculate the microstrain.

The crystallite sizes (as shown in Table 1) given by the three different W.-H. methods are all around 30 nm, which is consistent with the signal palygorskite crystal shown in Figure 1. Among the three methods, the deviation given by the average (LANGFORD) method is always smaller than other two methods. Although the classic linear method also provides a small deviation, the deviation increases sharply when analysing the samples with larger microstrain, such as the 10 s and 220 s samples. This shows that the classic linear method is not suitable for estimating the crystallite sizes of samples with microstrain. It also shows that the palygorskite powder prepared after mechanical grinding do have some microstrain. Therefore, this paper adopts the average method

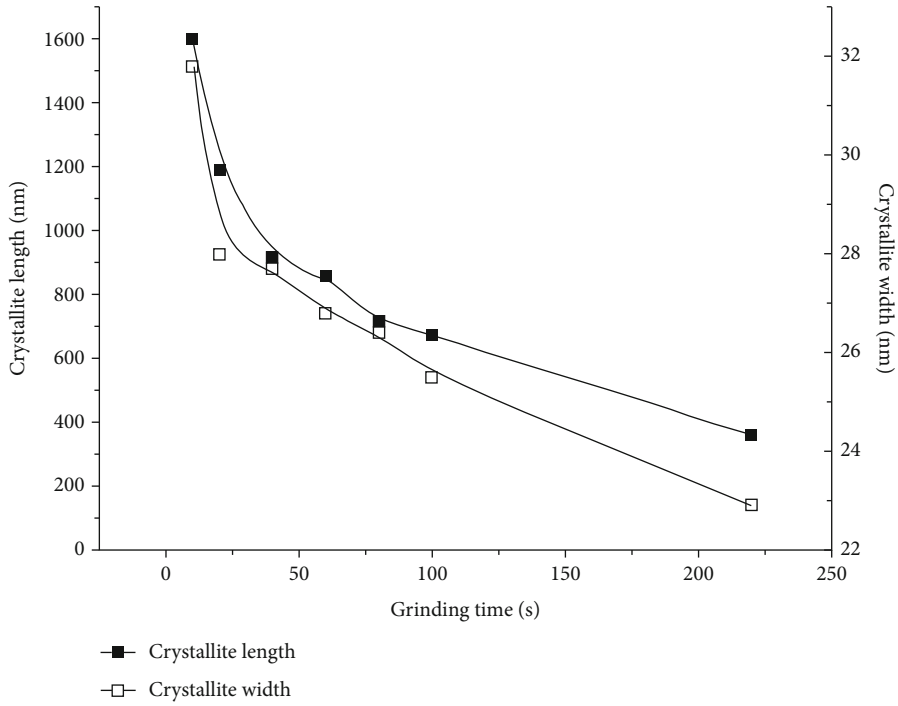

Figure 5: Crystallite size of palygorskite at different grinding time (■ is the crystallite length estimated by DLS, □ is the crystallite width estimated by XRD).

(LANGFORD method) to estimate the crystallite sizes of palygorskite.

3.2. DLS. The purified palygorskite samples were ground by high-speed vibration mill. In this paper, samples produced under seven different grinding times were selected for DLS detection. In order to explore the grinding limit, the grinding time of the last sample increased by 600% (120 s) compared with the previous. The grinding time, 220 s, is close to the limit time of a continuous grinding of the mill.

The corresponding relation between grinding time and particle size is shown in Table 2 and Figure 5. The figure shows that, in the first 40 s, the samples were significantly ground, and the particle size of 40 s sample was 43.31% lower than 10 s sample. With the increase of grinding time, the grinding efficiency decreased significantly, and the particle size of 100 s sample only decreased by 25.61% compared with 40 s sample. The figure together with the table shows that the longer the grinding time, the finer the particles, and the lower the grinding efficiency.

After 220 seconds of intense grinding, the particle sizes measured by DLS are still much longer than 50 nm. Compared with the TEM picture of palygorskite crystals shown in Figure 1, the particle sizes of palygorskite estimated by DLS are not the width values. As known, the DLS method can effectively measure the rotation radius of the particle [22]. Palygorskite is a kind of rod-like crystal, so the rotation radius represented by DLS method can be considered as the length of palygorskite crystals, which is the l value of Equation (1).

3.3. Calculation of Aspect Ratio. The primary size (l) of the crystal is given by DLS, and the secondary size (w) of the crystal is given by XRD analysis. The aspect ratios of the crystals under different grinding time can be calculated by using Equation (1). The results are shown in Table 2 and Figure 5, which shows that the aspect ratio of palygorskite can be effectively reduced by means of mechanical grinding. With the lengthening of grinding time, the aspect ratio of palygorskite decreased from 50.30 at 10 s to 15.70 at 220 s.

TEM images of palygorskite crystals at different grinding times are shown in Figure 6. From the images, it can be seen that the length of palygorskite crystals gradually decreases with the extension of grinding time, while the width of crystals decreases weakly. However, due to the limitations of TEM, it is difficult to find single palygorskite crystal in the view field. For example, the photo of "false single crystal" is shown in Figure 6(g), which is composed of two closely connected crystals.

The reason for the sharp decrease of aspect ratio can be attributed to the characteristics of palygorskite crystals. Palygorskite is a kind of crystal that grows in the direction of c-axis in the chain, and its regular crystal shapes are long rod-like in the direction of a-axis. Mechanical grinding makes it easier to break the long bar crystal and turn it into short bar crystal. However, the effect of mechanical grinding on the width of the crystals is much lower, which makes the aspect ratio of palygorskite crystals shows a trend of sharp decline in the extension of grinding time.

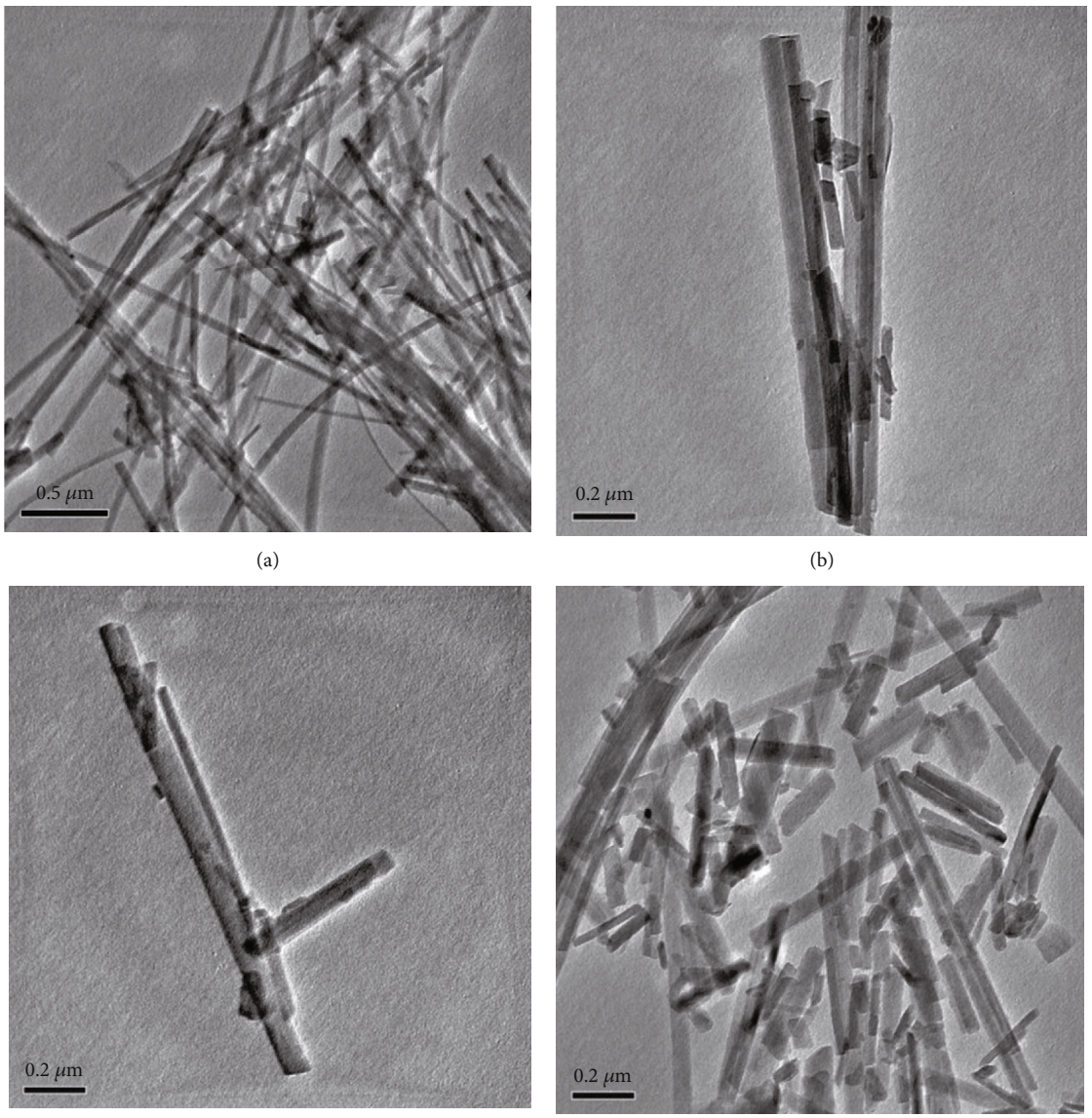

Figure 6: Continued.

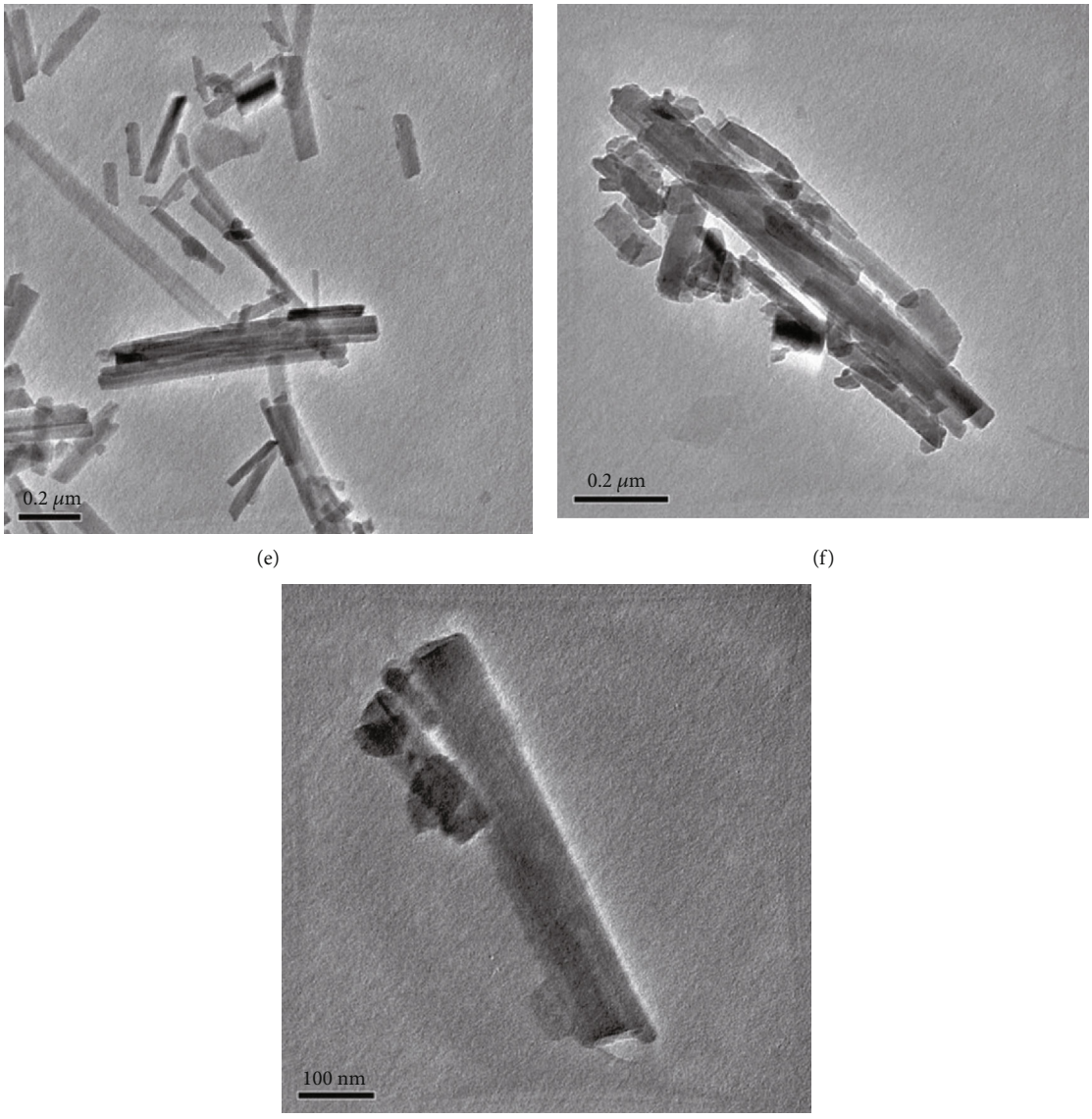

Figure 6: TEM images of palygorskite crystals under different grinding times((a) grinding time is 10 s; (b) grinding time is 20 s; (c) grinding time is 40 s; (d) grinding time is 60 s; (e) grinding time is 80 s; (f) grinding time is 100 s; (g) grinding time is 220 s).

4. Conclusion

(1) In this paper, the advantages of DLS and XRD testing techniques are comprehensively utilized to accurately obtain the length and width, so as to accurately calculate the length-diameter ratio of palygorskite

(2) The aspect ratio calculated in this paper is the average value of a huge number of particles, so it is more reliable than the conventional methods

(3) The proper parameter for W.-H. analysis of palygorskite should be Pearson VII function, Caglioti equation, and average (LANGFORD) method

(4) The aspect ratio of palygorskite sharply decreases with the grinding time. When subjected to mechanical stress, palygorskite crystals are more prone to fracture in the *a*-axis direction and less prone to wear in the *c*-axis direction

Data Availability

Some or all data, models, or code generated or used during the study are available from the author, Xie fei, email 83445651@qq.com, by request.

Conflicts of Interest

The authors declare that they have no conflicts of interest.

Acknowledgments

This study is supported by the National Natural Science Foundation of China for Creative Research Groups (Grant

nos. 41862002 and 51164004) and Joint Funds of Department of Science & Technology of Guizhou Province and Guizhou University (Grant no. LH [2016]7462).

References

[1] C. BALTAR, A. DALUZ, L. BALTAR, C. DEOLIVEIRA, and F. BEZERRA, "Influence of morphology and surface charge on the suitability of palygorskite as drilling fluid," *Applied Clay Science*, vol. 42, no. 3-4, pp. 597–600, 2009.

[2] W. Pabst, E. Gregorová, and C. Berthold, "Particle shape and suspension rheology of short-fiber systems," *Journal of the European Ceramic Society*, vol. 26, no. 1-2, pp. 149–160, 2006.

[3] H. Yin, D. Mo, and D. Chen, "Orientation behaviour of attapulgite nanoparticles in poly(acrylonitrile)/attapulgite solutions by rheological analysis," *Journal of Polymer Science. Part B*, vol. 47, no. 10, pp. 945–954, 2009.

[4] H. Yang, A. Tang, J. Ouyang, M. Li, and S. Mann, "From natural attapulgite to mesoporous materials: methodology, characterisation and structural evolution," *The Journal of Physical Chemistry B*, vol. 114, no. 7, pp. 2390–2398, 2010.

[5] L. Shi, J. Yao, J. Jiang, L. Zhang, and N. Xu, "Preparation of mesopore-rich carbons using attapulgite as templates and furfuryl alcohol as carbon source through a vapor deposition polymerization method," *Microporous and Mesoporous Materials*, vol. 122, no. 1-3, pp. 294–300, 2009.

[6] T. Chen, "Direct evidence of transformation from smectite to paly-gorskite: TEM investigation," *Science in China Series D*, vol. 47, no. 11, pp. 985–994, 2004.

[7] H. H. Murray, "Traditional and new applications for kaolin, smectite, and palygorskite a general overview," *Applied Clay Science*, vol. 17, no. 5-6, pp. 207–221, 2000.

[8] B. Pan, J. Ren, Q. Yue, B. Liu, J. Zhang, and S. Yang, "Interfacial interactions and performance of polyamide 6/modified attapulgite clay nanocomposites," *Polymer Composites*, vol. 30, no. 2, pp. 147–153, 2009.

[9] B. Xu, W. M. Huang, Y. T. Pei et al., "Mechanical properties of attapulgite clay reinforced polyurethane shape-memory nanocomposites," *European Polymer Journal*, vol. 45, no. 7, pp. 1904–1911, 2009.

[10] J. Gao, Q. Zhang, K. Wang et al., "Effect of shearing on the orientation, crystallization and mechanical properties of hdpe/attapulgite nanocomposites," *Composites Part A Applied Science and Manufacturing*, vol. 43, no. 4, pp. 562–569, 2012.

[11] B. R. Jennings and K. Parslow, "Particle size measurements: the equivalent spherical diameter," *Proceedings of the Royal Society of London. A. Mathematical and Physical Sciences*, vol. 419, pp. 139–149, 1988.

[12] W. Hohenberger, "Fillers and reinforcements," in *Plastics Additives Handbook*, H. Zweifel, Ed., pp. 901–948, Hanser Publishers, Munich, 2001.

[13] W. Pabst, C. Berthold, and E. Gregorová, "Size and shape characterization of oblate and prolate particles," *Journal of the European Ceramic Society*, vol. 27, no. 2-3, pp. 1759–1762, 2007.

[14] D. Gantenbein, J. Schoelkopf, G. P. Matthews, and P. A. C. Gane, "Determining the size distribution-defined aspect ratio of rod-like particles," *Applied Clay Science*, vol. 53, no. 4, pp. 538–543, 2011.

[15] C. Baerlocher, L. B. McCusker, and L. Palatinus, "Charge flipping combined with histogram matching to solve complex crystal structures from powder diffraction data," *Zeitschrift für Kristallographie*, vol. 222, no. 2, pp. 47–53, 2007.

[16] K. Venkateswarlu, A. Chandra Bose, and N. Rameshbabu, "X-ray peak broadening studies of nanocrystalline hydroxyapatite by Williamson-Hall analysis," *Physics B*, vol. 405, no. 20, pp. 4256–4261, 2010.

[17] V. Soleimanian and M. Mojtahedi, "A comparison between different X-ray diffraction line broadening analysis methods for nanocrystalline ball-milled FCC powders," *Applied Physics A*, vol. 119, no. 3, pp. 977–987, 2015.

[18] H. I. Gharsallah, T. Makhlouf, J. Saurina et al., "Effect of boron addition on structural and magnetic properties of nanostructured fe75al25 alloy prepared by high energy ball milling," *Materials Letters*, vol. 181, pp. 21–24, 2016.

[19] E. Tomaszewska, K. Soliwoda, K. Kadziola et al., "Detection limits of dls and uv-vis spectroscopy in characterization of polydisperse nanoparticles colloids," *Journal of Nanomaterials*, vol. 2013, 10 pages, 2013.

[20] G. Gelardi, N. Sanson, G. Nagy, and R. Flatt, "Characterization of comb-shaped copolymers by multidetection sec, dls and sans," *Polymers*, vol. 9, no. 12, p. 61, 2017.

[21] B. Chu and T. Liu, "Characterization of nanoparticles by scattering techniques," *Journal of Nanoparticle Research*, vol. 2, no. 1, pp. 29–41, 2000.

[22] S. Khouri, M. Shams, and K. C. Tam, "Determination and prediction of physical properties of cellulose nanocrystals from dynamic light scattering measurements," *Journal of Nanoparticle Research*, vol. 16, no. 7, 2014.

[23] S. Takabumi and U. Takatsugu, "Occurrences and mineralogical properties of long-fibrous palygorskite from Guizhou Province, China," *Clay Science*, vol. 45, no. 3, pp. 200–210, 2006.

[24] T. Degen, M. Sadki, E. Bron, U. König, and G. Nénert, "The HighScore suite," *Powder diffraction*, vol. 29, no. S2, pp. S13–S18, 2014.

[25] G. Chiari, R. Giustetto, and G. Ricchiardi, "Crystal structure refinements of palygorskite and maya blue from molecular modelling and powder synchrotron diffraction," *European Journal of Mineralogy*, vol. 15, no. 1, pp. 21–33, 2003.